Electronic supplementary information

Orthogonal solvent-sequential deposition of nonfullerene acceptor solution on polymer donor film: complete interpenetration and highly efficient inverted organic solar cells†

Haizhen Liu,‡ Zesheng Zhang,‡ Dong Yuan,‡ Mingqing Chen, Haiying Jiang, Jiahao Liang, Xing Chen, Di Sun, Lianjie Zhang, Linlin Liu, Yuguang Ma and Junwu Chen*

Institute of Polymer Optoelectronic Materials & Devices, State Key Laboratory of Luminescent Materials & Devices, South China University of Technology, Guangzhou 510640, P. R. China. E-mail: psjwchen@scut.edu.cn

† Electronic supplementary information (ESI) available. See DOI:10.1039/xxxxx

‡ These authors contributed equally to this article.

Experimental Section

Materials

PFN-Br was purchased from Solarmer Materials (Bejing) Inc. Polymer donors Si25, PQSi705 and D18-C16 were synthesized according to previous reports.[1-3] Non-fullerene acceptors Y6-HD and Y6-BO were purchased from Shenzhen Yirou Photovoltaic Technology Co., Ltd. The processing solvents used in the device fabrication were purchased from Sigma Aldrich and used as received.

Device fabrication

The devices with a 0.057 cm^2 active area were fabricated in both conventional and

inverted structures. A conventional device structure of indium tin oxide (ITO)/poly (3,4-ethylenedioxythiophene) polystyrene sulfonate (PEDOT:PSS)/active layer/PFN-Br/Al and an inverted one of ITO/ZnO/active layer/MoO3/Al were utilized in this work. The patterned ITO-coated glass substrates with a sheet resistance of 15-20 ohm square^{-1} were cleaned by sequential sonication using detergent, acetone, deionized water, and ethanol, and dried in oven at 70 ℃ before used.

For the conventional devices, PEDOT:PSS (Baytron P VP AI 4083 from H. C. Stark) was spin-coated on top of pre-cleaned and UVO-treated ITO substrate at 3000 rpm for 30 s, and then dried at 150 ℃ for 15 min in air. Subsequently, the ITO substrates were transferred to a nitrogen-filled glovebox and then the donor and acceptor solutions were spin-coated on the substrates. For sequentially deposited Si25/Y6-HD active layer, the Si25 was dissolved in chlorobenzene with 6 mg/mL at 80 ℃ and then spin-coated with the hot solution, leading to a Si25 layer with a thickness of about 50 nm. A 8 mg/mL Y6-HD solution dissolved in chloroform was spin-coated on the Si25 layer at 1500 rpm, and the thickness of the Y6-HD layer was about 55nm. For Si25:Y6-HD BHJ active layer, Si25:Y6-HD blend solution were prepared by dissolving in 80 ℃ chlorobenzene at a donor concentration of 6 mg/mL with a donor:acceptor mass ratio of 1:1.2. The spin-coating film of BHJ active layer was conducted at 1500 rpm for 60 s, giving a film thickness of ~105 nm. For the D18-C16/Y6-BO SD active layer, the D18-C16 was dissolved in indane with 6 mg/mL at 60 ℃ and was spin-coated at 1600 rpm to form a film of about 50 nm. A 8 mg/mL Y6-BO solution dissolved in tetrahydrofuran was spin-coated on the D18-C16 layer at 1500 rpm. The thickness of

the Y6-BO layer was about 55 nm. Then the active layer was annealed at 100 ℃ for 10 min. For the PQSi705/Y6-BO SD active layer, the PQSi705 was dissolved in *o*-xylene with 10 mg/mL at 60 ℃. The PQSi705 solution was spin-coated on the substrate at 1800 rpm to form a film of about 50 nm. A 8 mg/mL Y6-BO solution dissolved in tetrahydrofuran was spin-coated on the PQSi705 layer at 1500 rpm. The thickness of the Y6-BO layer was about 55 nm. Subsequently, the PQSi705/Y6-BO SD active layer was annealed at 110 ℃ for 5 min. Afterward, around 5 nm thick PFN-Br layer (0.5 mg/mL in methanol, 2000 rpm) was spin-coated onto the active layer. Finally, 100 nm aluminum (Al) was thermally deposited through a shadow mask in a vacuum chamber at a pressure of 2×10^{-4} Pa.

For the inverted devices, a ZnO layer of 30 nm was spin-coated onto the ITO substrate and annealed at 200 ℃ on a hot plate for 30 min. After that, the ITO substrates were transferred to a nitrogen-filled glove-box and the active layer was spin-coated on the substrates. The preparation methods of the Si25/Y6-HD SD active layer, Si25:Y6-HD BHJ active layer, D18-C16/Y6-BO SD active layer, and PQSi705/Y6-BO SD active layer are same as those for the conventional devices. Finally, 5 nm MoO_3 and then 100 nm Al were thermally deposited on top of the active layer through a shadow mask in a vacuum chamber at a pressure of 2×10^{-4} Pa.

Instruments and characterization

UV-vis absorption spectra were carried out via UV-3600 (Shimadzu Co.) spectrophotometer.

The thickness values of the PEDOT:PSS, ZnO, PFN-Br, and active layer were

verified by a surface profilometer (Tencor, Alpha-500), and the thickness values of the evaporated MoO_3 and Al cathodes were monitored by a quartz crystal thickness/ratio monitor (Model: STM-100/MF, Sycon).

The Gel permeation chromatography (GPC): The molecular weights of Si25, PQSi705 and D18-C16 were determined using a PL-GPC 220 high-temperature chromatography in 1,2,4-trichlorobenzene (TCB) at 150 ℃ and using a calibration curve of polystyrene standards.

The photovoltaic performance was measured under an AM 1.5G (air mass 1.5 global) spectrum from a solar simulator (Japan, SAN-EI, XES-40S1). The light intensity of the solar simulator was calibrated with standard silicon solar cell at 100 mW/cm^2 before the testing, the silicon solar cell was calibrated by a National Renewable Energy Laboratory (NREL) certified silicon photodiode. The current density-voltage (*J-V*) curves were recorded with a Keithley 2400 source meter.

The external quantum efficiency (EQE) data were gained through the solar-cell spectral-response measurement system (QE-R3011，Enlitech), which was calibrated with a crystal silicon photovoltaic cell before testing.

The hole mobilities (μ_h) and electron mobilities (μ_e) of active layers were measured by the space charge limited current (SCLC) method[4] with hole-only devices of ITO/PEDOT:PSS/Active layer/MoO_3/Al and electron-only devices of ITO/ZnO/Active layer/PFN-Br/Al. The μ_h and μ_e were determined by fitting the dark current to the model of a single carrier SCLC, described by the equation:

$$J = \frac{9}{8}\varepsilon_0\varepsilon_r\mu\frac{V^2}{d^3}$$

where J is the current, ε_0 is the permittivity of free space, ε_r is the material relative permittivity, V is the effective voltage and d is the thickness of the active layer. The effective voltage can be obtained by subtracting the built-in voltage (V_{bi}) from the applied voltage (V_{appl}), $V=V_{appl} - V_{bi}$. The mobility can be calculated from the slope of the $J^{1/2}$ -V curves.

The surface morphologies of AFM images relative to the corresponding SD and BHJ active layers were obtained on a Multimode 8 Dimension Icon Scanning Probe Microscope (Bruker, Multimode 8) in the tapping mode.

TEM micrographs of the SD and BHJ active layers were obtained on a JEM 1400 Plus microscope operating at 300kV.

Time-of-Flight Secondary Ion Mass Spectrometry (TOF-SIMS) Measurements. The depth-profile data were obtained with TOF-SIMS (ION-TOF GmbH, Germany) instrument in negative mode (sputter condition: a 5 kV GCIB beam; 45deg; Area: 400 µm ×400 µm; analysis condition: a 30 keV Bi3+ beam; 45deg; Area: 150 µm×150 µm; Pixel 128*128).

Supplementary Figures and Tables

Table S1 Photovoltaic device parameters and processing conditions of active layer prepared for inverted SD OSCs

Donor	Solvent (D)	Acceptor	Solvent (A)	V_{OC} [V]	J_{SC} [mA cm^{-2}]	FF [%]	PCE [%]	Ref.
PCPDTFBT	o-XY	PC$_{71}$BM	*o*-XY:DCB	0.71	16.4	50	5.84	[5]
PffBT4T-2OD	CB:DCB	PC$_{71}$BM	CB:DCB	0.76	16.5	75	9.4	[6]
PBDB-T	CB	IT-IC	*o*-XY	0.86	15.30	50.50	6.70	[7]
J60	CB	TBDPDI-C$_5$	CB	0.969	10.57	59.62	6.11	[8]
Si25	CB	Y6-HD	CF	0.70	24.85	67.52	11.74	**This work**
PQSi705	o-XY	Y6-BO	THF	0.84	25.49	72.61	15.57	**This work**
D18-C16	Indane	Y6-BO	THF	0.89	26.99	67.57	**16.23**	**This work**
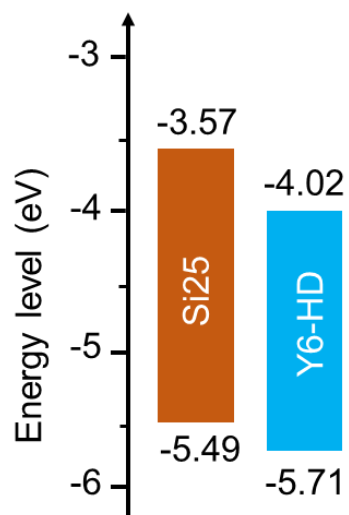
Fig. S1 The energy levels of polymer Si25 and acceptor Y6-HD. The energy levels of the Si25 were obtained from cyclic voltammetry results, which carried out on a CHI660A electrochemical workstation.[9] The energy levels of the Y6-HD were based on literature.[10]
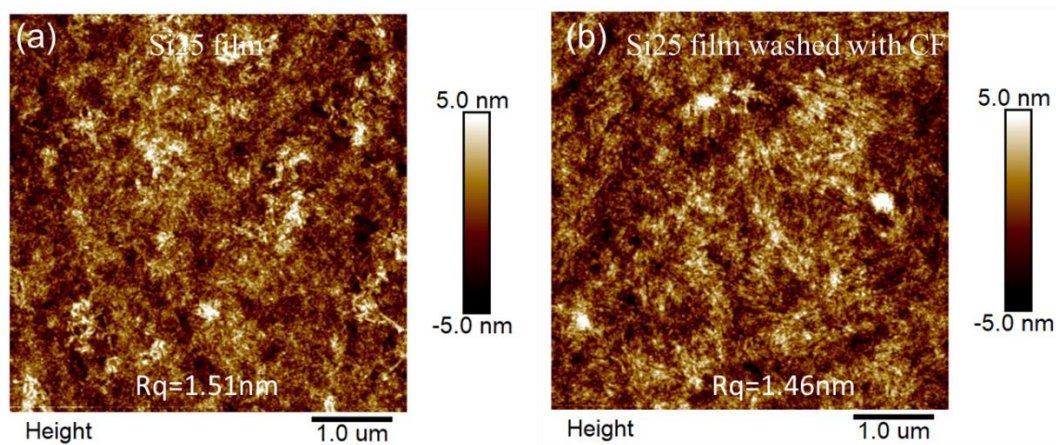
**Fig. S2** AFM images of the (a) Si25 film and (b) its film washed with chloroform.
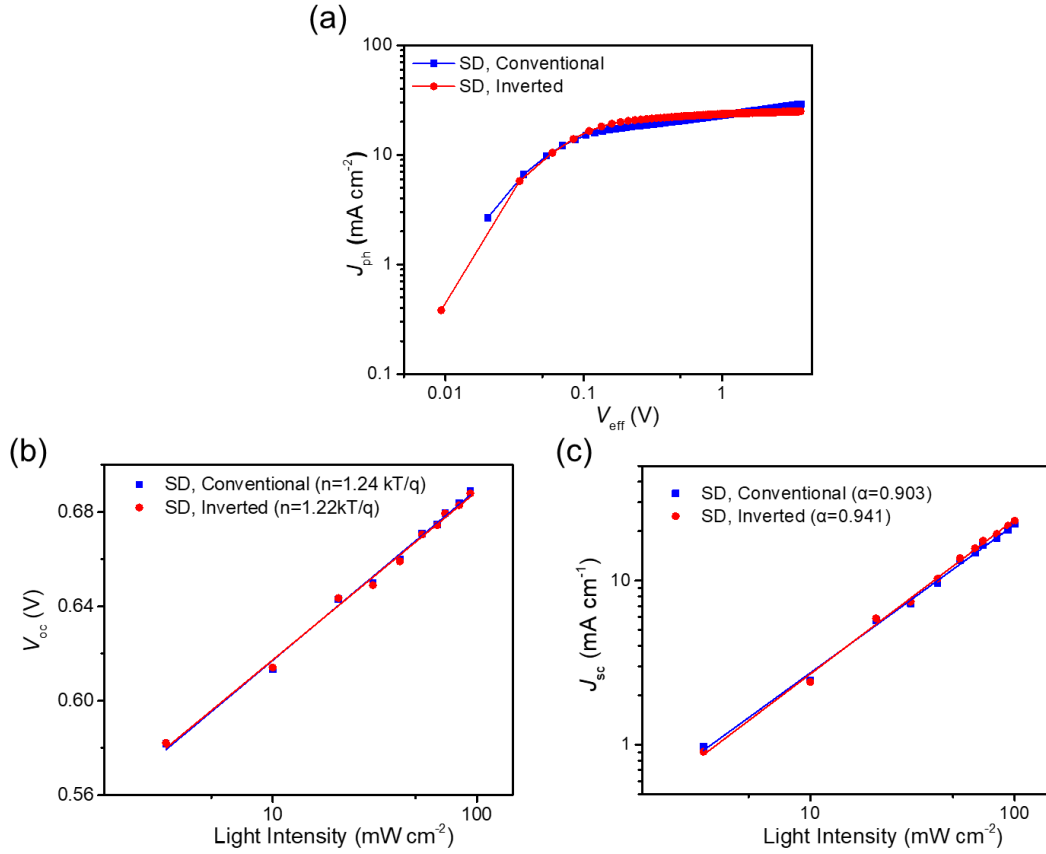
Fig. S3 (a) J_{ph}-V_{eff} curves and (b) the dependency of V_{oc} on light intensity and (c) J_{sc} on light intensity of the OSCs based on Si25/Y6-HD SD active layer.

Table S2 J_{ph}, J_{sat}, dissociation efficiency (η_{diss}) and charge collection efficiency (η_{coll}) of the devices based on Si25/Y6-HD SD active layer
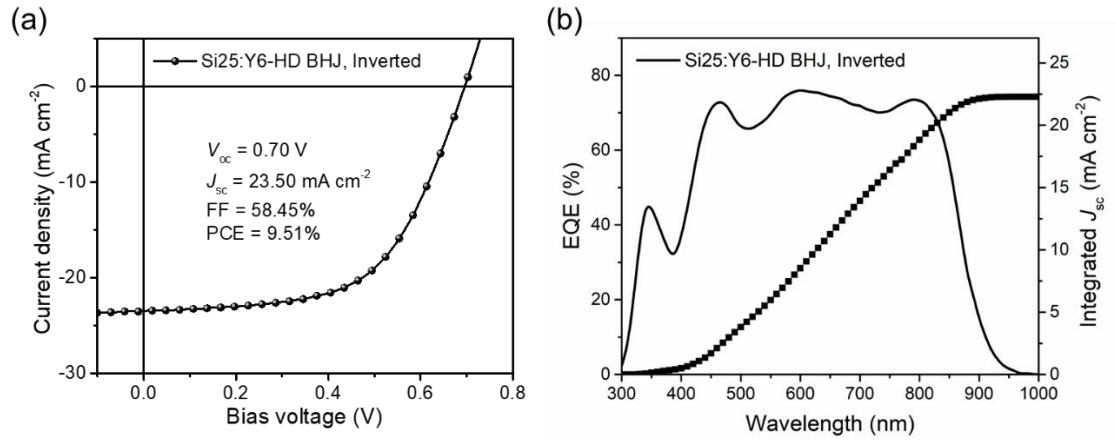
Device structure	J_{ph} [a] [mA/cm^2]	J_{ph} [b] [mA/cm^2]	J_{sat} [mA/cm^2]	η_{diss} [%]	η_{coll} [%]
Conventional	22.58	18.15	23.27	97.03	77.99
Inverted	23.77	19.82	24.50	97.02	80.89

[a] J_{ph} under short-circuit condition. [b] J_{ph} under maximal power output condition.
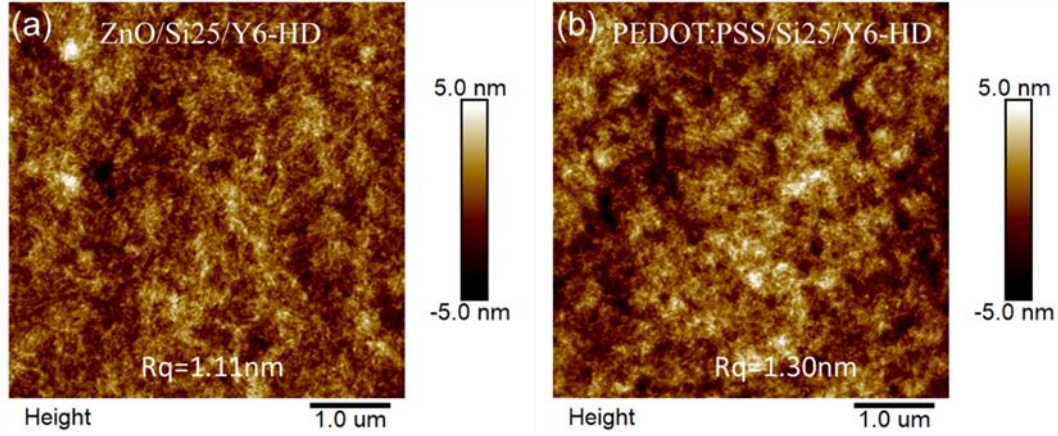
**Fig. S4** AFM images of the Si25/Y6-HD SD active layer spin coating on (a) ZnO and (b) PEDOT:PSS substrate.

Fig. S5 (a) The current density-voltage (*J-V*) curve and (b) EQE curves of Si25:Y6-HD based BHJ active layer inverted devices.

Table S3. Performance parameters of the inverted BHJ OSCs based on the Si25:Y6-HD active layers

| Device structure	V_{OC} [V]	J_{SC} [mA cm^{-2}]	$J_{sc,EQE}$ [mA cm^{-2}]	FF [%]	PCE[a] [%]
Inverted	0.70	23.50	22.32	58.45	9.51
	(0.70 ±0.004)	(22.99 ±0.70)		(57.13 ±0.97)	(9.18 ±0.28)

[a] Statistical data in parentheses are average values with standard deviation from 10 independent devices.
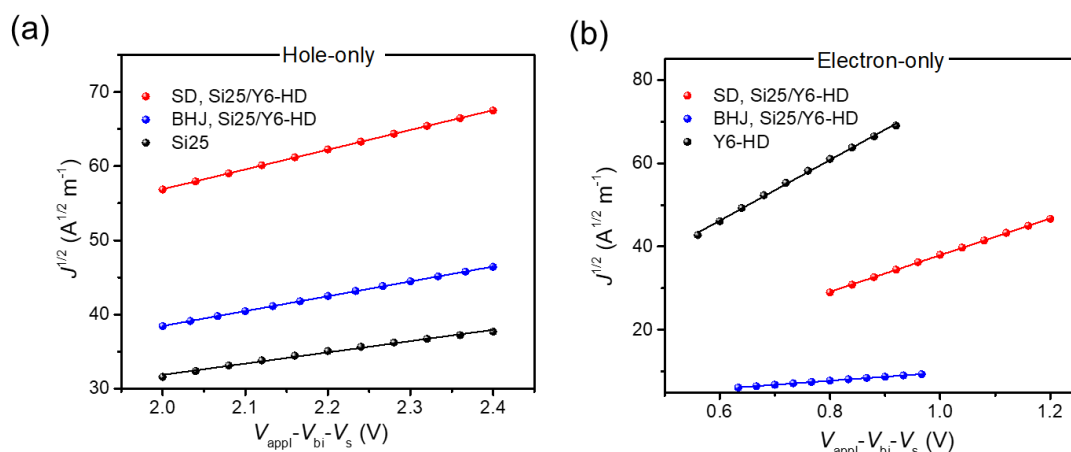
Fig. S6 $J^{1/2}$-V curves of the (a) hole-only based on Si25 neat film as well as Si25/Y6-HD SD and Si25:Y6-HD BHJ active layer, and (b) electron devices based on Y6-HD neat film as well as Si25/Y6-HD SD and Si25:Y6-HD BHJ active layer.

Table S4. The hole mobilities (μ_h) and electron mobilities (μ_e) values of Si25, Y6-HD neat film as well as the Si25/Y6-HD SD and Si25:Y6-HD BHJ active layer.

Device	hole mobility (μ_h)	electron mobility(μ_e)	μ_e / μ_h
Si25	2.60×10^{-4}	/	/
Y6-HD	/	7.49×10^{-4}	/
SD, Si25/Y6-HD	5.23×10^{-4}	1.43×10^{-3}	2.73
BHJ, Si25:Y6-HD	4.54×10^{-4}	1.05×10^{-4}	4.32
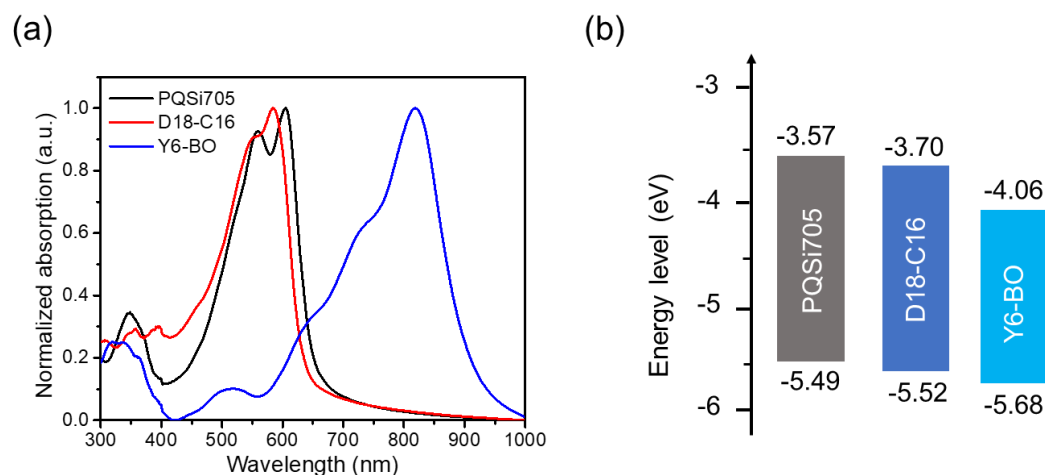
Fig. S7 (a) The film absorption spectra and (b) energy levels of PQSi705, D18-C16 and Y6-BO. The energy levels of the PQSi705 and D18-C16 were obtained from cyclic voltammetry results, which carried out on a CHI660A electrochemical workstation.[9] The energy levels of the Y6-HD were based on literature.[11]
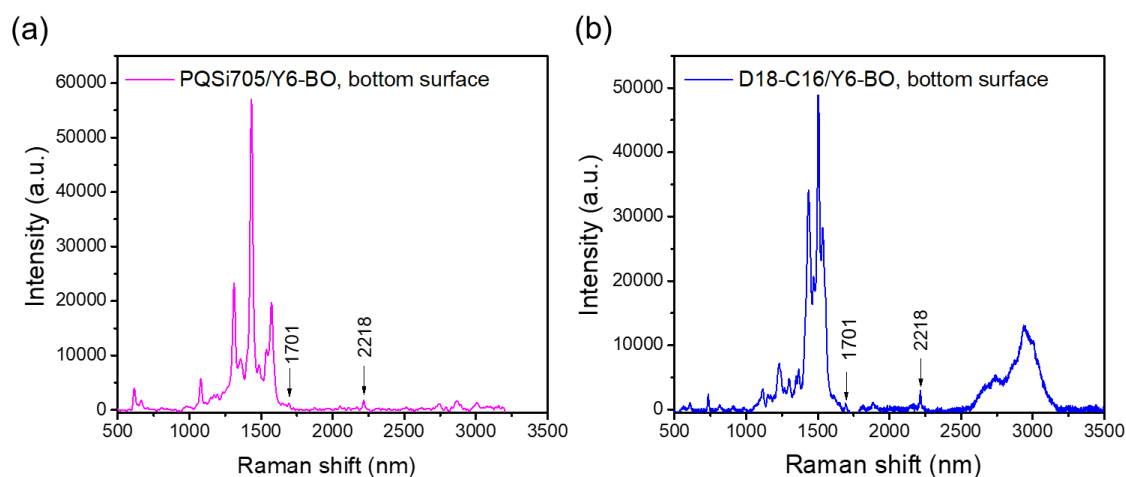
Fig. S8 Raman spectra of the bottom surface of PQSi705/Y6-BO and D18-C16/Y6-BO SD film.

References

1. X. Liu, L. Nian, K. Gao, L. Zhang, L. Qing, Z. Wang, L. Ying, Z. Xie, Y. Ma, Y. Cao, F. Liu and J. Chen, *J. Mater. Chem. A*, 2017, **5**, 17619-17631.

2. D. Yuan, L. Zhang and J. Chen, *ChemSusChem*, 2022, **15**, e202200789.

3. Q. Liu, Y. Jiang, K. Jin, J. Qin, J. Xu, W. Li, J. Xiong, J. Liu, Z. Xiao, K. Sun, S. Yang, X. Zhang and L. Ding, *Sci. Bull.*, 2020, **65**, 272-275.

4. M. A. Lampert and P. Mark, *Electrical Science*, 1970, **21**, 558.

5. C. Lang, J. Fan, Y. Zhang, F. Guo and L. Zhao, *Org. Electron.*, 2016, **36**, 82-88.

6. S. Dong, K. Zhang, B. Xie, J. Xiao, H.-L. Yip, H. Yan, F. Huang and Y. Cao, *Adv. Energy Mater.*, 2019, **9**, 1802832.

7. L. Huang, P. Jiang, Y. Zhang, L. Zhang, Z. Yu, Q. He, W. Zhou, L. Tan and Y. Chen, *ACS Appl. Mater. Interfaces*, 2019, **11**, 26213-26221.

8. M. Hu, Y. Zhang, X. Liu, X. Zhao, Y. Hu, Z. Yang, C. Yang, Z. Yuan and Y. Chen, *ACS Appl. Mater. Interfaces*, 2021, **13**, 29876-29884.

9. X. Yuan, H. Chen, S. Kim, Y. Chen, Y. Zhang, M. Yang, Z. Chen, C. Yang, H. Wu, X. Gao, Z. Liu and C. Duan, *Adv. Energy Mater.*, 2023, **13**, 2204394.

10. Z. Abbas, S. U. Ryu, M. Haris, C. E. Song, H. K. Lee, S. K. Lee, W. S. Shin, T. Park and J.-C. Lee, *Nano Energy*, 2022, **101**, 107574.

11.   L. Hong, H. Yao, Z. Wu, Y. Cui, T. Zhang, Y. Xu, R. Yu, Q. Liao, B. Gao, K. Xian, H. Y. Woo, Z. Ge and J. Hou, *Adv. Mater.*, 2019, **31**, 1903441.